The emergence of optical elastography in biomedicine

Brendan F. Kennedy[1,2], Philip Wijesinghe[1,3], and David D. Sampson[3,4]

[1]BRITElab, Harry Perkins Institute of Medical Research, QEII Medical Centre, 6 Verdun Street, Nedlands, WA 6009, Australia

[2]School of Electrical, Electronic & Computer Engineering, The University of Western Australia, 35 Stirling Highway, Perth, WA 6009, Australia

[3]Optical+Biomedical Engineering Laboratory, School of Electrical, Electronic & Computer Engineering, The University of Western Australia, 35 Stirling Highway, Perth, WA 6009, Australia

[4]Centre for Microscopy, Characterisation & Analysis, The University of Western Australia, 35 Stirling Highway, Perth, WA 6009, Australia

Optical elastography, the use of optics to characterise and map the mechanical properties of biological tissue, involves measuring the deformation of tissue in response to a load. Such measurements may be used to form an image of a mechanical property, often elastic modulus, with the resulting mechanical contrast complementary to the more familiar optical contrast. Optical elastography is experiencing new impetus in response to developments in the closely related fields of cell mechanics and medical imaging, aided by advances in photonics technology, and through probing the micro-scale between that of cells and whole tissues. Two techniques have shown particular promise recently: optical coherence elastography and Brillouin microscopy; for medical applications, such as in ophthalmology and oncology, and as new techniques in cell mechanics.

At every length scale, the mechanical properties of tissue are important. Mechanical and chemical interactions at the molecular and cellular level are fundamentally interwoven in determining biological function, and such interactions and related mechanical properties play an important role in the onset and progression of many diseases, including eye disease, cancer, and atherosclerosis[1,2]. Over the past 25 years, a range of elastography techniques have been developed to image the mechanical properties of tissue[3]. Elastography is now a commercial medical imaging technique, mainly finding application as a diagnostic tool in the assessment of liver fibrosis[4], and of breast cancer[5]. Primarily based on ultrasonography or magnetic resonance imaging, such elastography provides images, known as elastograms, over centimetre to whole-body depth ranges, at millimetre-scale spatial resolutions far lower than is possible with optics. At higher resolutions, on the cellular scale, the measurement of mechanical properties underpins the field of cell mechanics[2], which is focussed on understanding cellular-scale mechanical properties and how cells respond to physical forces and the mechanical properties of their environment. Cell mechanics is supported by nano- and micro-imaging techniques, such as atomic force microscopy (AFM) and traction force microscopy[6].

Optical elastography is at a much earlier stage of development than the methods employed in medical imaging or in cell mechanics. It is ideally positioned to image mechanical properties on the intermediate scale, between that of cells and organs[7-8], which presents new opportunities in the understanding, diagnosis and treatment of disease[6]. The use of optics in elastography offers the combination of micro-scale imaging, potential for *in vivo* deployment and high sensitivity to variations in mechanical properties, and holds promise for a wide range of applications in areas such as oncology, ophthalmology and cell mechanics. Many optical elastography techniques have been proposed, for example, based on optical coherence tomography[7-9], Brillouin microscopy[10], laser speckle[11], ultrasound-modulated optical tomography[12] and digital holography[13]. In this Progress article, we restrict our focus to new,

emerging methods that have demonstrated the greatest advances over the last five years, namely, those based on optical coherence tomography (OCT)[7-9], termed optical coherence elastography (OCE), and Brillouin microscopy[10], and briefly compare them to the most prominent of the many other available approaches.

Probing the mechanical properties of tissue using optics dates back to at least the 1950s[14]. Surface techniques, such as holography and electronic speckle pattern interferometry, have long been used to measure the mechanical properties of hard tissues, such as bone[15]. The extension to form sub-surface images of soft tissue based on mechanical contrast began in 1998, with the work of Schmitt[9], who saw the opportunity to utilize the high-resolution and depth-penetrating characteristics of OCT to detect depth-resolved sample deformation induced by quasi-static compression. Around the same time, the use of laser speckle imaging on soft tissue, a surface optical elastography technique, also began to be explored[11]. After a flurry of early demonstrations[7], progress slowed, limited by the available imaging technology. OCE, for example, was based on the time-domain OCT systems available at that time, with insufficient imaging speed and sensitivity to tissue deformation to produce high quality or three-dimensional (3D) images. The onset of Fourier-domain OCT[16] reinvigorated OCE, with a range of new techniques and applications proposed over the last five years[7-8]. In Fourier-domain OCT, the scanning mirror used to obtain depth sectioning in time-domain OCT is replaced by a static mirror and detection of the spectral interference fringes, the inverse Fourier transform of which provides depth sectioning. This innovation has led to significantly higher acquisition speeds and displacement sensitivity required for OCE. In parallel, driven by the availability of ultra-high (spectral) resolution imaging spectrometers, Brillouin microscopy[10,17] has also advanced over a similar time frame. These two techniques have led to the development of a vibrant new area of imaging, at the interface between optics and mechanics. Here, we present

an overview of recent developments in optical elastography and describe the open challenges in translating recent progress into applications across medicine and the life sciences.

Optical elastography techniques

OCE in its various forms and Brillouin microscopy probe different frequency ranges of mechanical properties: common configurations of emerging optical elastography techniques and the frequency ranges they probe are shown in Fig. 1. Here, we focus on their technical aspects, and in the next section consider applications in medicine and biology.

Optical coherence elastography

OCT, based on low-coherence interferometry[18], typically achieves spatial resolutions of ~5-15 μm, determined, in the axial direction, by the coherence of the optical source and, in the lateral direction, by the width of the focussed beam. Combining interferometry with lateral beam scanning, OCT provides rapid 3D image acquisition: volumes of dimensions 10×10×2 mm can be acquired in <1 second. To perform OCE, a mechanical load is applied to the tissue and the resulting deformation is usually measured using either speckle tracking or phase-sensitive detection[7], described below. The loading mechanisms broadly fit into the same categories as for elastography in general: compression, harmonic, or transient[7-8], which we now consider in turn.

Most of the initial work on OCE was based on compressive loading[9] (Fig. 1a) and such techniques remain prominent (see Fig. 2[19]). Compressive loading is typically applied step-wise and quasi-statically, *i.e.*, at sufficiently low rates (typically <50 Hz) that no detectable wave propagation is induced. The resulting measured local strain in the tissue, defined as the gradient of displacement with depth, is mapped into an elastogram[7]. Although strain is a relative quantity, under the simplest assumption that the load imparts uniform stress throughout the

sample, strain is inversely proportional to elastic modulus (the ratio of stress to strain). Strain is a tensor quantity, yet in most cases in OCE, not all components of the tensor are measured, as discussed further below. In the setup used to generate Fig. 2, for example, only the axial component is measured. The spatial resolution of compression OCE is often reported, in the lateral dimensions, as the resolution of the underlying OCT system and, in the axial dimension, as the range used to estimate strain at each pixel, typically 15-100 μm[7].

Compression loading of the whole area of interest provides a practical means of imaging over a wide field-of-view, and the opportunity to perform rapid 3D imaging: volumes have been acquired in as little as 5 seconds[20]. Measuring only strain, or equivalently, assuming uniform stress throughout the sample, restricts the contrast to being a relative quantity. To move towards a quantitative measurement of elastic modulus, a variation on the compression technique has recently been proposed in which imaging is performed through a compliant, transparent reference layer, the deformation of which is used to estimate the axial stress at each point in the lateral plane at the tissue surface[21]. The stress, along with strain at the sample surface, is used to estimate Young's modulus. Fig. 2l shows strong contrast, improved by a factor of 100 over the associated strain image (not shown).

OCE can also be performed based on dynamic forms of loading. One approach is to apply a continuous single-tone sinusoidal modulation, via a contact transducer or an acoustic wave, to induce harmonic tissue motion. The harmonic load may be localised, as illustrated in Fig. 1b, or applied across the entire sample, analogously to compression OCE, but at higher frequency. Under steady state conditions and in the presence of boundaries on the centimetre scale, the resulting reflections may cause the formation of standing waves in tissue samples at the resonant frequencies of the sample, which can be experimentally determined by scanning the load frequency[22,23]. Such harmonic techniques make use of boundary reflections that, by

contrast, other techniques seek to avoid. This feature may be of benefit when imaging organs such as the eye or eardrum. The challenge, though, is that the measured resonance is likely to be influenced as much by the sample's structure and boundaries as by its mechanical properties, requiring intimate knowledge of the sample geometry to effectively decouple the mechanical parameters. Additionally, local vibration amplitude generated by local or whole-tissue loading across a spectrum of frequencies, often termed spectroscopic OCE, can be used to generate images of mechanical contrast, and provide insight into the viscoelasticity of tissue[24].

An alternative dynamic approach, inspired by related techniques in ultrasound elastography[25], is to impart a transient (pulsed) localised load to excite an acoustic wave in the tissue (Fig. 1c). Various implementations have been proposed, based on contact with an indenter, or non-contact air jets, laser pulses, and acoustic radiation force[7-8]. Examples of their application in the cornea[26] and retina[27] are shown in Fig. 3. An important feature of transient techniques is that the elastic modulus is estimated directly from the acoustic phase velocity measured using OCT[28]: The square root of the elastic modulus is proportional to the phase velocity of the sample under the assumptions of uniform density and known Poisson's ratio[7,8]. The nature of the acoustic wave propagation and, hence, the precise relationship to elastic modulus, is dependent on the sample geometry and how the wave is excited. Propagation is described differently for different depths and in the presence of layers: close to the tissue surface is described as surface acoustic waves[28]; propagation within thick tissues is described as shear waves[25]; and propagation in a layered medium is described as Lamb waves[26]. Large fields of view are challenging to achieve in transient OCE. To ensure reflections at boundaries are not encountered and to avoid problems related to the decay of shear waves with propagation distance, the load must often be scanned across the tissue surface. Transient techniques can, thus, be time-consuming, making challenging their application to time-sensitive applications, such as *in vivo* imaging. This challenge is being overcome, to some extent, through the use of

high-speed Fourier-domain mode-locked lasers in swept-source OCT systems. Such an OCT system has recently been used to demonstrate OCE at 1.5 million depth scans (A-scans) per second[29].

Displacement detection approaches: To measure the deformation induced by the mechanical load with OCT, two main methods have been used: speckle tracking or phase-sensitive detection[7]. In speckle tracking, the cross-correlation of consecutive 2D[30] or 3D images[31] acquired under different mechanical loading is often used to estimate displacement. Speckle tracking was used in many of the early demonstrations of OCE[9] and is still prominent, particularly using full-field OCE[30,31], where there is not ready access to the phase of the detected signal. An advantage of speckle tracking over phase-sensitive detection is its ability to measure 3D displacement, and its lower sensitivity to motion artefact, potentially important for *in vivo* applications; however, its spatial resolution is lower than the native OCT resolution, because of the need for a window over which to perform the cross-correlation (typically of dimensions 4-5× the OCT resolution). Its dynamic range of measurable displacement is limited by the speckle size at the lower limit and by the decorrelation of speckle for displacements greater than ~0.5× the OCT resolution at the upper limit. To overcome this limitation, a technique has been developed to estimate strain directly from speckle decorrelation[32].

The onset of Fourier-domain detection in OCT has afforded the opportunity to track nanometre-scale displacements because of the ready access it provides to the interferometric optical phase[16]. Such phase-sensitive detection was used to produce the results shown in Fig. 2 and Fig. 3. For a sample subjected to mechanical loading that causes an axial displacement between two line-scans (A-scans) acquired from the same lateral position, the measured phase shift, $\Delta\phi$, is related to the axial displacement, u_z, by $u_z = \Delta\phi\lambda / 4\pi n$ [33], where λ is the mean wavelength of the source and n is the average refractive index along the beam path. The displacement

sensitivity using phase-sensitive detection is limited by shot noise and, with averaging, can be as low as 10s of picometres[7]. Displacements that produce a phase difference of greater than 2π (corresponding to a displacement of ~0.5 μm at a wavelength of 1,300 nm) are confounded by phase wrapping, limiting the maximum measurable displacement. However, this maximum can be extended, assuming speckle remains correlated, by using phase unwrapping algorithms[34]. These characteristics of phase-sensitive detection provide a dynamic range of measurable displacement far larger than achievable with speckle tracking. However, the majority of phase-sensitive techniques measure only the axial component of displacement. Measurement of the lateral displacement components as well (as done in MR elastography) would represent a more complete mechanical characterization and, therefore, be expected to increase the accuracy of optical elastography. It is, thus, likely that phase-sensitive Doppler OCT techniques[35] or advanced 3D speckle decorrelation methods for measuring lateral flow will be translated to OCE in the coming years.

Brillouin microscopy

Brillouin scattering, first reported in 1922, is the inelastic scattering of light by gigahertz-frequency acoustic waves (phonons) intrinsic to a material[10]. The (up or down) frequency shift, υ_B, of the Brillouin scattered light is given by $\upsilon_B = \frac{2\upsilon_0 n}{c} V \sin\left(\frac{\theta}{2}\right)$, where υ_0 is the illumination frequency, c is the speed of light, n is the local refractive index, θ is the angle between the incident and scattered light and V is the acoustic velocity, which is related to the Brillouin, or longitudinal, modulus, M (defined as the ratio of stress to strain in a uniaxial strain state) by $M = \rho V^2$, where ρ is the density. Brillouin spectroscopy of liquids has been practised since the 1960s, but its advance as a practical imaging method required the development of a high-performance imaging

spectrometer capable of sub-gigahertz spectral resolution: the virtually imaged phased array (VIPA). Scarcelli and Yun first demonstrated imaging with this device in 2008[10], and the field of Brillouin microscopy (Fig. 1d) has begun to blossom[10,17,36-41]. A particular advantage of Brillouin microscopy has been its capacity for high spatial resolution (as high as 1.5 μm and 0.3 μm in the axial and transverse directions, respectively[17]), achieved using a high numerical aperture imaging lens[36]. When combined with the features of being non-contact and the absence of extrinsic mechanical loading, it appears particularly well suited to applications in cell mechanics[37] and ophthalmology[38-40]. Figure 4a shows Brillouin microscopy images of the spatially resolved longitudinal modulus within a cell and Fig. 4b shows *in vivo* results acquired from a patient with keratoconus.

A complication in the estimation of the longitudinal modulus is that the density and refractive index of the sample are not usually known, introducing uncertainty. (The issue of unknown density also affects shear-wave OCE, and the issue of unknown refractive index affects all axial displacement measurements in OCE). A more critical challenge is to quantify the relationship between the longitudinal modulus and the mechanical parameters commonly used by biologists, such as elastic modulus, measured using techniques such as AFM and OCE. The longitudinal modulus is related to the elastic modulus, E, by $M = \frac{E(1-\nu)}{(1+\nu)(1-2\nu)}$, where ν is the Poisson's ratio. In incompressible materials, where ν approaches 0.5, M approaches infinity. In soft tissue, ν can often be between 0.499 and 0.4999, resulting in M being more than 5 orders of magnitude greater than E. Indeed, this was observed by Scarcelli *et al.*[38]; however, the measured relationship between M and E was not constant, suggesting that either ν varied in proportion with E or, more likely, that phonons at gigahertz frequencies are subject to viscoelastic effects. Reliably quantifying the relationship between M and E will represent a further important advance in this new window into a previously unobserved regime of tissue

and cell mechanics. An issue for *in vivo* applications of Brillouin microscopy is the long acquisition times, typically several seconds for an axial line, corresponding to ~20 minutes for 3D measurements[40]. Recently, the first use of stimulated scattering in Brillouin microscopy has been published, which is proposed to significantly reduce the acquisition time[41].

Resolution in optical elastography is determined principally by three factors: the resolution of the underlying imaging system; the model used to estimate the mechanical property, for example, the strain fitting range in compression OCE; and the structural and mechanical properties of the tissue. The first two factors are generally known, are sample independent and, in keeping with the convention adopted in all forms of elastography, are used to define resolution in this article. The third factor leads to the local mechanical behaviour being dependent not only on the tissue's local mechanical properties but on the mechanical and structural properties of the surrounding tissue regions and boundaries. As a result, the true resolution in an elastogram of heterogeneous tissue is likely to be spatially varying. In all forms of elastography that aim to quantify an absolute mechanical property, this third factor may only be effectively taken into account through numerical computation, which we discuss later.

Table 1 shows the key performance metrics of OCE and Brillouin microscopy, compared to those of magnetic resonance elastography, ultrasound elastography and AFM. The ranges used for the various metrics reflect the anticipated or typical values in each case, rather than the best reported values. A main advantage of optical elastography techniques over currently used elastography techniques in medical imaging is their higher resolution. In addition, optical elastography systems are readily miniaturised, opening the possibility to provide small footprint probes, for example, in endoscopic and needle formats. This feature, as well as high acquisition speeds, and sub-surface and wide-area probing, differentiates optical elastography from the higher resolution AFM. A main limitation of optical elastography in comparison to

both magnetic resonance elastography and ultrasound elastography is the limited penetration depth (typically several millimetres at most).

Applications

There are many opportunities to utilise optical elastography in biological and medical applications and, in particular, to exploit its micro-scale resolution and millimetre-to-centimetre range, sitting between cellular imaging and whole tissues, its non-contact capability and potential for *in vivo* use. To date, the majority of publications have represented proof-of-principle demonstrations of a particular technique. More advanced feasibility studies demonstrating the potential of optical elastography have begun to emerge in a number of areas, most notably in oncology[19,42], ophthalmology[38-40] and cell mechanics[30,37].

Oncology: It is well established that cancer modifies tissue mechanical properties on length scales from the cellular to the whole organ level; indeed, elastic modulus, qualitatively assessed using palpation, is commonly used to locate tumours prior to and during surgery. Early work in OCE demonstrated its potential to distinguish tumour[43]. Application of optical elastography intraoperatively has the potential to more accurately identify malignant tissue than with existing tools. For example, in breast-conserving surgery, by scanning the margins of excised tumour masses and/or the tumour cavity, optical elastography has the potential to help surgeons reduce the incidence of residual tumour remaining after surgery[19]. A recent demonstration of compression OCE in breast cancer, shown in Fig. 2[19], has shown the promise of heterogeneous mechanical contrast as a signature of tumour in solid tissue, with much greater contrast than possible with OCT alone. In prostate cancer, a study has demonstrated the potential of optical elastography in differentiating malignant and non-malignant tissue biopsies[42].

Ophthalmology: Optical elastography has the potential to assess a range of conditions in the eye and to date has been used in assessment of the cornea and lens. In the cornea, keratoconus causes bulging due to the reduction in mechanical integrity brought about by disruption of the collagen matrix. A new form of ultraviolet light therapy to stiffen the cornea through collagen cross-linking can be monitored by optical elastography[39]. Age-related stiffening of the crystalline lens is thought to be the primary cause of presbyopia and is also implicated in the onset of cataracts, the leading cause of blindness in the world. Both OCE[26,44] and Brillouin microscopy[38,40] have recently demonstrated the potential to assess the mechanical properties of the cornea and the lens. If further refinements and larger studies lead to translation, they have the potential to significantly improve the treatment of patients with these conditions.

Cell mechanics: The increased (or reduced) ability of cells to deform is central in diseases such as cancer and malaria. Tools, such as AFM and traction force microscopy[6], have been used to probe cell mechanics and have provided insights into such diseases. One limitation is that existing tools are difficult to use on whole tissues or in living systems and are often limited to cell cultures or *ex vivo* measurement of the surface cell layer. Another is that a cell responds to mechanical cues, such as the forces imparted by surrounding cells and the extracellular matrix. To observe such behaviour accurately requires cells to be in their native 3D environment[6]. High-resolution optical elastography has the potential to address these issues, as shown by recent demonstrations of full-field OCT[30], ultra-high resolution OCE[45] and Brillouin microscopy[37]. Another interesting prospect is to mechanically load cells using magnetic micro-particles, as has been demonstrated using a high-resolution OCT system[46].

Optical elastography may also impact on other applications areas, including in: cardiology, as an intravascular tool to image the mechanical properties of atherosclerotic plaque[17,23]; dermatology, as a tool for scar assessment; and tissue engineering, to characterise the elastic modulus of biomaterials. The application in cardiology is particularly interesting, because of

the scale of the potential impact and the difficulty of the challenge. OCE[23], Brillouin microscopy[17] and laser speckle-based elastography[47] have all been proposed to measure the elastic modulus of atherosclerotic plaques. However, the advance of optical elastography in cardiology will require the development of intravascular probes to allow suspicious plaques to be interrogated *in vivo*.

Challenges and outlook

The understanding of mechanical contrast in optical elastography, and its similarities and differences to the more familiar optical contrast, remains at a very early stage, with much still likely to be discovered. Optical elastography has made great recent technical advances that have allowed demonstrations in the applications described above, with each technique having attributes making it suited to particular applications. In the delicate cornea, the non-contact nature of Brillouin microscopy and of transient OCE is an important attribute. In breast tumour margin assessment, a large surface area (up to ~5×5 cm) must be scanned rapidly and there is no issue with contacting the tissue, which suits compression OCE. Such diverse application requirements ensure that many different variations of optical elastography will continue to be developed.

Overall, few techniques have reached the maturity or scale needed for translation. In ophthalmology, although great technical strides have been made, only a few studies have demonstrated the technique in living tissue[38,40]. The translation of OCE to routine *in vivo* application faces the challenge of overcoming motion artefact. As optical elastography relies on accurate measurement of nano- to micro-scale displacements, it is especially sensitive to user and/or patient motion. The potential of optical elastography in cardiology highlights a more general impediment in accelerating applications: the lack of compact imaging probes

capable of accessing tissue *in situ*. Such probes face the challenge of combining loading and imaging in a compact format. Some progress has been made, for example, in demonstrating optical elastography at centimetre depths in tissue with interstitial (needle-based) probes[48].

Many demonstrations have been restricted to showing mechanical contrast without being able to reliably quantify the mechanical property of interest, either through the method being intrinsically limited, for example, strain imaging, or due to unknown tissue parameters, such as density. Such quantification is needed for many applications, for example, if a mechanical property is to be compared in the same tissue over time or between different tissues. The models of tissue deformation used to estimate the elastic modulus, thus far, have been simplified by necessity to allow for a simple closed-form solution[3]. For instance, tissue is typically assumed to be mechanically homogeneous. The ready generation of elastograms enabled by these models, however, is accompanied by image artefacts when tissue deformation deviates from the ideal. Many of the artefacts are related to unaccounted for boundary conditions, particularly at the tissue surface. Surface artefacts are much less prominent in ultrasound elastography and magnetic resonance elastography, where the tissue surface has less effect owing to their higher penetration. Surface effects manifest differently in each optical elastography technique. In compression techniques, friction between the mechanical loading plate and the tissue surface restricts the lateral expansion of the tissue at the boundary during loading, resulting in a higher measured elastic modulus. In transient techniques, the presence of the tissue boundary makes it challenging to decouple surface waves from shear waves propagating in the bulk material.

The higher complexity of models that are more faithful to non-uniform, complex soft tissue mechanics will invariably necessitate the use of numerical computation to extract the mechanical properties. A promising avenue to address challenges in accurately measuring elastic modulus lies in developing computational solutions to the inverse elasticity problem, a direction that is actively being explored in all forms of elastography, including recently in

optical elastography[49]. Such computational approaches treat tissue deformation with fewer assumptions and, thus, have the potential to remove the influence of the internal structure (including mechanical interconnection) and boundaries of a sample on the accuracy and resolution. Computational approaches bring with them their own set of factors to be considered in interpreting elastograms. Numerical solutions to the inverse elasticity problem have a high computational overhead, are susceptible to noise[49] and still rely on assumed values of parameters such as refractive index, density and Poisson's ratio.

Additionally, consistent with the broader field, optical elastography techniques typically treat tissue as a linear elastic material. However, in general, soft tissue is nonlinear and viscoelastic. As a result, the majority of optical (and non-optical) elastography techniques measure only one aspect of a tissue's mechanical properties, typically Young's modulus. Techniques that incorporate a more complete viscoelastic model are expected to increase in prominence, as they will lead not only to a more accurate quantification of tissue mechanical properties, but may provide new contrast. Already a number of techniques have been developed to measure the viscoelasticity of tissue[47], as recently reviewed[50].

Optical elastography has greatly advanced in the last few years, yet the journey is just beginning. The next challenge lies in translating proof-of-principle demonstrations into compelling biological and clinical applications. As momentum continues to gather, efforts must be focussed on pushing these technologies beyond the confines of optics laboratories and into the hands of those who will put them to work: biologists, medical researchers and clinicians.

References

1 Cowin, S. C. & Doty, S. B. *Tissue Mechanics*. (Springer, 2007).
2 Janmey, P. A. & McCulloch, C. A. Cell mechanics: integrating cell responses to mechanical stimuli. *Annu. Rev. Biomed. Eng.* 9, 1-34 (2007).
3 Parker, K. J., Doyley, M. M. & Rubens, D. J. Imaging the elastic properties of tissue: the 20 year perspective. *Phys. Med. Biol.* **56**, R1-R29 (2011).
4 Jaffer, O. S., Lung, P. F. C., Bosanac, D., Shah, A. & Sidhu, P. S. Is ultrasound elastography of the liver ready to replace biopsy? A critical review of the current techniques. *Ultrasound* **20**, 24-32 (2012).
5 Wojcinski S. *et al.* Multicenter study of ultrasound real-time tissue elastography in 779 cases for the assessment of breast lesions: Improved diagnostic performance by combining the BI-RADSR - US classification system with sonoelastography," *Ultraschall Med.*, **31**, 484–491 (2010).
6 Lee, G. Y. & Lim, C. T. Biomechanics approaches to studying human diseases. *Trends Biotechnol.* **25**, 111-118 (2007).
7 Kennedy, B. F., Kennedy, K. M. & Sampson, D. D. A review of optical coherence elastography: fundamentals, techniques and prospects. *IEEE J. Sel. Top. Quant.* **20**, 272-288 (2014).
8 Wang, S. & Larin, K. V. Optical coherence elastography for tissue characterization: a review. *J. Biophotonics* **8**, 279-302 (2015).
9 Schmitt, J. M. OCT elastography: imaging microscopic deformation and strain of tissue. *Optics Express* **3**, 199-211 (1998).
10 Scarcelli, G. & Yun, S. H. Confocal Brillouin microscopy for three-dimensional mechanical imaging. *Nat. Photonics* **2**, 39-43 (2008).
11 Jacques, S. L. & Kirkpatrick, S. J. Acoustically modulated speckle imaging of biological tissues. *Opt. Lett.* **23**, 879-881 (1998).
12 Bossy, E. *et al.* Transient optoelastography in optically diffusive media. *Appl. Phys. Lett.* **90**, 174111 (2007).
13 Mohan, K. D. & Oldenburg, A. L. Elastography of soft materials and tissues by holographic imaging of surface acoustic waves. *Opt. Express* **20**, 18887-18897 (2012).
14 Von Gierke, H. E., Oestreicher, H. L., Franke, E. K., Parrack, H. O. & von Wittern, W. W. Physics of vibrations in living tissues. *J. Appl. Physiol* **4**, 886-900 (1952).
15 Orr, J. F. & Shelton, J. C. *Optical Measurement Methods in Biomechanics*. (Chapman & Hall, 1997).
16 Leitgeb, R., Hitzenberger, C. & Fercher, A. Performance of Fourier domain vs. time domain optical coherence tomography. *Opt. Express* **11**, 889-894 (2003).
17 Antonacci, G. *et al.* Quantification of plaque stiffness by Brillouin microscopy in experimental thin cap fibroatheroma. *J. R. Soc. Interface* **12**, 20150843 (2015).
18 Huang, D. *et al.* Optical coherence tomography. *Science* **254**, 1178-1181 (1991).
19 Kennedy, B. F. *et al.* Investigation of optical coherence microelastography as a method to visualize cancers in human breast tissue. *Cancer Res.* **75**, 3236-3245 (2015).
20 Kennedy, B. F., Malheiro, F. G., Chin, L. & Sampson, D. D. Three-dimensional optical coherence elastography by phase-sensitive comparison of C-scans. *J. Biomed. Opt.* **19**, 076006 (2014).
21 Kennedy, K. M. *et al.* Quantitative micro-elastography: imaging of tissue elasticity using compression optical coherence elastography. *Sci. Rep.* **5**, 15538 (2015).

22 Qi, W. *et al.* Resonant acoustic radiation force optical coherence elastography. *Appl. Phys. Lett.* **103**, 103704 (2013).
23 Akca, B. I. *et al*. Observation of sound-induced corneal vibrational modes by optical coherence tomography. *Biomed. Opt. Express*. **6**, 3313-3319 (2015).
24 Adie, S. G. *et al.* Spectroscopic optical coherence elastography. *Opt. Express* **18**, 25519-25534 (2010).
25 Sarvazyan, A. P., Rudenko, O. V., Swanson, S. D., Fowlkes, Emelianov, S. Y. Shear wave elasticity imaging: A new ultrasonic technology of medical diagnostics. *Ultrasound Med. Biol.* **24**,1419-1435 (1998).
26 Wang, S. & Larin, K. V. Noncontact depth-resolved micro-scale optical coherence elastography of the cornea. *Biomed. Opt. Express* **5**, 3807-3821 (2014).
27 Song, S., Le, N. H., Huang, Z., Shen, T., & Wang, R. K. Quantitative shear-wave optical coherence elastography with a programmable phased array ultrasound as the wave source. *Opt. Lett*. **40**, 5007-5010 (2015).
28 Li, C., Guan, G., Cheng, X., Huang, Z. & Wang, R. K. Quantitative elastography provided by surface acoustic waves measured by phase-sensitive optical coherence tomography. *Opt. Lett.* **37**, 722-724 (2012).
29 Singh, M., Wu, C., Liu, C-H., Li J., Schill A., Nair A. & Larin K. V. Phase-sensitive optical coherence elastography at 1.5 million A-Lines per second. *Opt. Lett*. **40**, 2588-2591 (2015).
30 Leroux, C-E., Palmier, J., Bocarra, A. C., Cappello, G. & Monnier, S. Elastography of multicellular aggregates submitted to osmo-mechanical stress. *N. J. Phys.* **17**, 073035 (2015).
31 Nahas, A., Bauer, M., Roux, S. & Boccara, A. C. 3D static elastography at the micrometer scale using Full Field OCT. *Biomed. Opt. Express* **4**, 2138-2149 (2013).
32 Zaitsev, V. Y., Matveev, L. A., Matveyev, A. L., Gelikonov, G. V. & Gelikonov, V. M. Elastographic mapping in optical coherence tomography using an unconventional approach based on correlation stability. *J. Biomed. Opt.* **19**, 021107 (2014).
33 Wang, R. K., Ma, Z. & Kirkpatrick, S. J. Tissue Doppler optical coherence elastography for real time strain rate and strain mapping of soft tissue. *Appl. Phys. Lett.* **89**, 144103 (2006).
34 Kennedy, B. F. *et al.* Optical coherence micro-elastography: mechanical-contrast imaging of tissue microstructure. *Biomed. Opt. Express* **5**, 2113-2124 (2014).
35 Bouwens, A., Szlag, D., Szkulmowski, M., Bolmont, T., Wojtkowski, M. & Lasser, T. Quantitative lateral and axial flow imaging with optical coherence microscopy and tomography. *Opt. Express*. **21**, 17711-17729 (2013).
36 Antonacci, G., Foreman, M. R., Paterson, C. & Torok, P. 2013. Spectral broadening in Brillouin imaging. *Appl. Phys. Lett*. **103**, 221105 (2013).
37 Scarcelli, G., Polacheck, W. J., Nia, H. T., Patel, K., Grodzinsky, A. J., Kamm, R. D. & Yun, S. H. Noncontact three-dimensional mapping of intracellular hydromechanical properties by Brillouin microscopy. *Nat Methods*. **12**, 1132-1136 (2015).
38 Scarcelli, G., Kim, P. & Yun, S. H. *In vivo* measurement of age-related stiffening in the crystalline lens by Brillouin optical microscopy. *Biophys. J.* **101**, 1539-1545 (2011).
39 Scarcelli, G. *et al.* Brillouin microscopy of collagen crosslinking: noncontact depth-dependent analysis of corneal elastic modulus. *Invest. Ophth. Vis. Sci.* **54**, 1418-1425 (2013).
40 Scarcelli, G., Besner, S., Pineda, R., Kalout, P. & Yun, S. H. *In vivo* biomechanical mapping of normal and keratoconus corneas. *JAMA Ophth*. **133**, 480-482 (2015).

41 Ballmann, C. W. *et al.* Stimulated Brillouin scattering microscopic imaging. *Sci. Rep*. **5**, 18139 (2015).
42 Li, C. *et al.* Detection and characterisation of biopsy tissue using quantitative optical coherence elastography (OCE) in men with suspected prostate cancer. *Cancer Lett.* **357**, 121-128 (2015).
43 Liang, X.; Oldenburg, A. L.; Crecea, V., Chaney, E. J.; Boppart, S. A. Optical micro-scale mapping of dynamic biomechanical tissue properties. *Opt. Express* **16,** 11052-11065 (2008).
44 Ford, M. R., Roy, A. S., Rollins, A. M., Dupps, W. J. Serial biomechanical comparison of edematous, normal, and collagen crosslinked human donor corneas using optical coherence elastography. *J. Cataract & Refr. Surg*. **40**, 1041-1047 (2014).
45 Curatolo, A. *et al*. Ultrahigh resolution optical coherence elastography. *Opt. Lett*. **41**, 21-24, 2015.
46 Crecea, V., Graf, B. W., Taewoo, K., Popescu, G., Boppart, S. A. High resolution phase-sensitive magnetomotive optical coherence microscopy for tracking magnetic microbeads and cellular mechanics. *IEEE J. Sel. Top. Quant.* **20**, 6800907 (2014).
47 Hajjarian, Z., Nadkarni, S. K. Evaluating the viscoelastic properties of tissue from laser speckle flucuations. *Sci. Rep.* **2**, 1-8 (2012).
48 Kennedy, K. M., Kennedy, B. F., McLaughlin, R. A. & Sampson, D. D. Needle optical coherence elastography for tissue boundary detection. *Opt. Lett.* **37**, 2310-2312 (2012).
49 Dong, L. *et al.* Quantitative compression optical coherence elastography as an inverse elasticity problem. *IEEE J. Sel. Top. Quantum Electron.* **22**, 6802211 (2016).
50 Mulligan, J. A., Untracht, G. R., Chandrasekaran, S. N., Brown, C. N. & Adie, S. G. Emerging approaches for high-resolution imaging of tissue biomechanics with optical coherence elastography," *IEEE J. Sel. Top. Quantum Electron.* **22**, 6800520 (2016).

Acknowledgements

The authors wish to thank their colleagues past and present who have contributed to the evolution of optical elastography; in particular, Steven Adie, Wes Allen, Lixin Chin, Andrea Curatolo, Shaghayegh Es'hagian, Kelsey Kennedy, Robert McLaughlin, and Peter Munro. This work has been supported in part by the Australian Research Council, and PW thanks the Schrader Trust for a studentship.

Figures

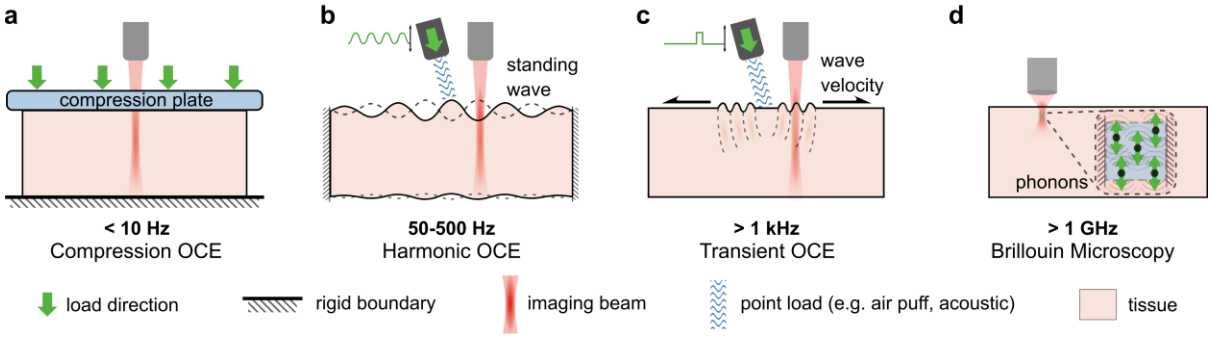

Figure 1 | Illustration of some emerging optical elastography techniques. a, Compression OCE. b, Harmonic OCE. c, Transient OCE. d, Brillouin microscopy. In each case, the typical mechanical frequencies being probed are given.

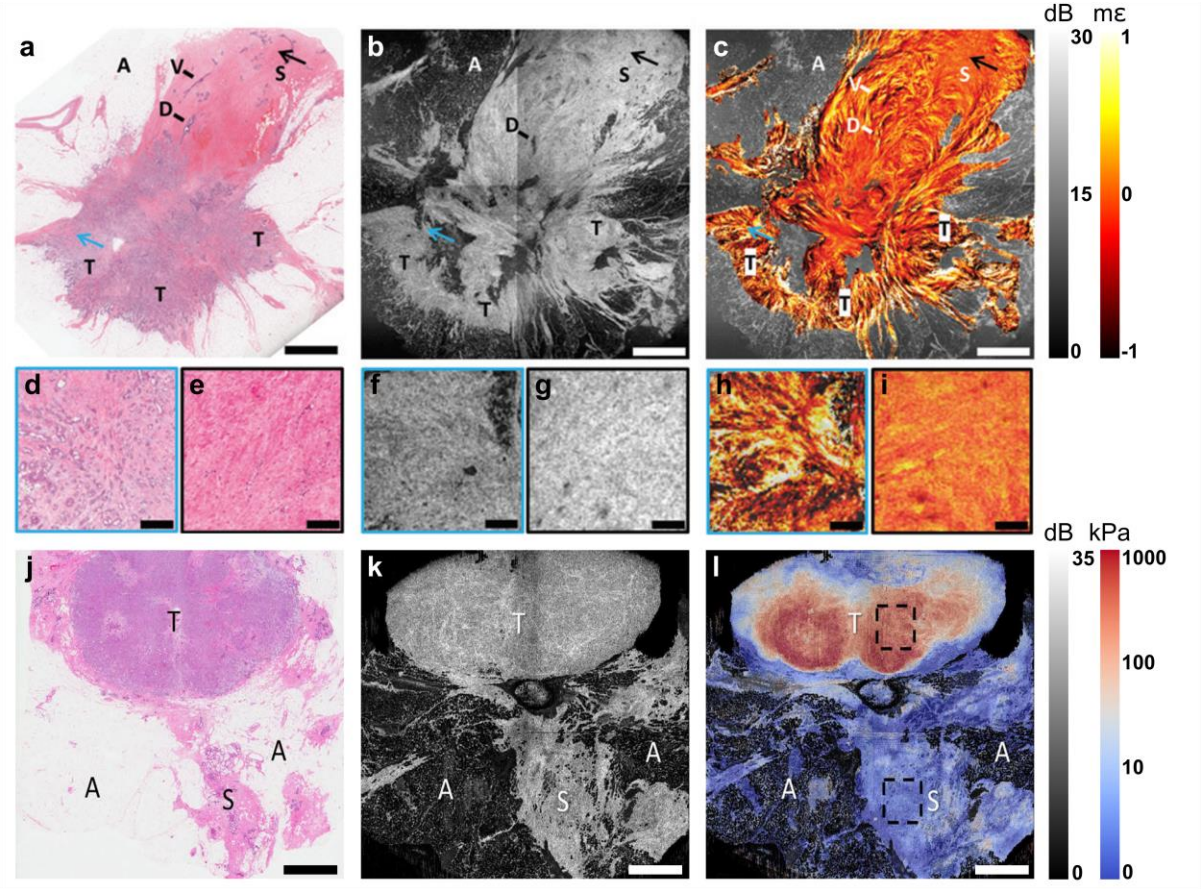

Figure 2 | Compression OCE showing strain (a-i) and elastic modulus (j-l) imaging of excised human breast tissue[19,21]. a, Histology corresponding to b, *en face* OCT image, and c, *en face*

OCT fused with elastogram (OCT in grey scale and OCE in false colour) at ~30 µm depth. d,f,h, Magnified regions of tumour indicated by blue arrows in a-c. e,g,i, Magnified regions of mature stroma indicated by black arrows in a-c. Tumour is readily identified in h by increased heterogeneity compared to i. j, Histology corresponding to k, *en face* OCT image, and l, *en face* OCT image fused with elastogram at ~30 µm depth. Tumour is identified by higher Young's modulus (logarithmic scale): 420 kPa in tumour and 5 kPa in stromal regions outlined by dashed boxes. Scale bars in a-c, j-l, 3 mm; in d-i, 0.5 mm. dB, decibels; mε, millistrain; kPa, kilopascals; A, adipose tissue; V, vessel; S, mature stroma; T, tumour.

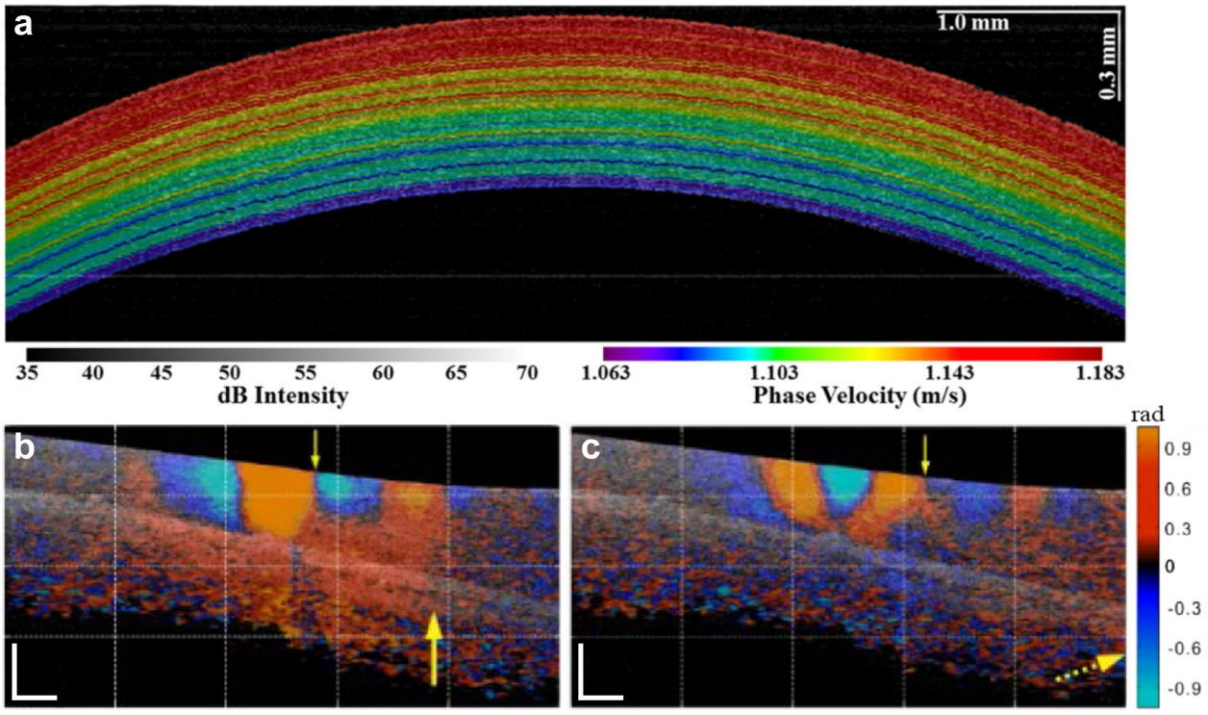

Figure 3 | Transient OCE of the eye. a, Two-dimensional map of an excised rabbit cornea showing the Lamb wave phase velocity[26]. The Lamb wave was generated using a micro-air puff to induce micro-scale transient deformation of the corneal surface. b,c, Shear waves generated in an excised porcine retina via a single acoustic radiation force impulse[27]. b and c show snapshots of the shear waves, respectively, 0.2 ms and 0.35 ms after the impulse. Shear wavefronts in the retina and the choroid are indicated by the small and large arrows,

respectively. In c, the dashed arrow indicates the wavefront in the choroid is beyond the field of view. Scale bar, 200 μm.

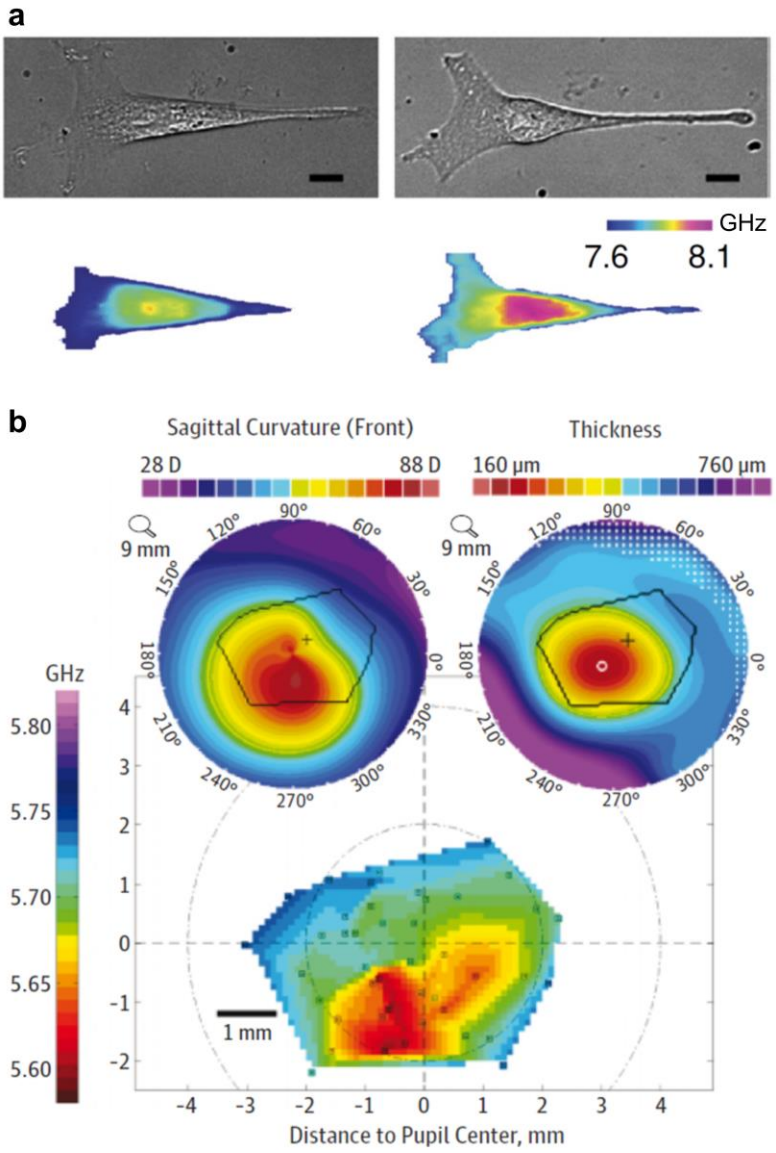

Figure 4 | Brillouin microscopy in cell mechanics and ophthalmology. a, Brillouin microscopy (lower panels) and co-registered phase-contrast microscopy (upper panels) images of an NIH 3T3 cell before and after hyperosmotic shock[37]. Colour bar represents Brillouin frequency shift in GHz. An increase in Brillouin frequency shift is observed after hyperosmotic shock. Scale bars, 10 μm. b, *In vivo* Brillouin microscopy (at bottom) on the cornea of a patient with advanced keratoconus[40]. Colour bar represents Brillouin frequency shift in GHz. Insets (at top)

are the respective sagittal curvature (D indicates diopters) and pachymetry (thickness) maps with outlined Brillouin-scanned areas. The keratoconic cornea presents strong spatial variations in Brillouin shift in comparison to the healthy cornea[40].

Materials & Correspondence

Please address correspondence and requests for materials to Brendan Kennedy Brendan.Kennedy@uwa.edu.au or David Sampson David.Sampson@uwa.edu.au.

Competing Financial Interests

OncoRes Medical Pty Ltd has recently been established to develop optical elastography for applications in breast-conserving surgery. BK and DS have shares in OncoRes Medical and in future BK will be undertaking funded research for this company.